Precision trace cas analysis by FT-IR spectroscopy. 1. Simultaneous analysis of CO2, CH4, N2O, and CO in air

ARTICLE *in* ANALYTICAL CHEMISTRY · JANUARY 2000

Impact Factor: 5.64 · DOI: 10.1021/ac9905625

4 AUTHORS, INCLUDING:

Michael Brian Esler
Research Statistics
17 PUBLICATIONS **460** CITATIONS
SEE PROFILE

Stephen R Wilson
University of Wollongong
89 PUBLICATIONS **869** CITATIONS
SEE PROFILE

Anal. Chem. **2000,** *72,* 206−215

Precision Trace Gas Analysis by FT-IR Spectroscopy. 1. Simultaneous Analysis of CO_2, CH_4, N_2O, and CO in Air

Michael B. Esler,*,† David W. T. Griffith,† Stephen R. Wilson,† and L. Paul Steele‡

Department of Chemistry, University of Wollongong, Wollongong NSW 2522, Australia, and CSIRO Atmospheric Research, Aspendale Vic 3195, Australia

We report the development of a method of trace gas analysis based on 1-cm^{-1} resolution Fourier transform infrared (FT-IR) spectroscopy, deployable in both laboratory and field applications. Carbon dioxide, methane, nitrous oxide, and carbon monoxide may be analyzed simultaneously in a single air sample using this method. We have demonstrated that the method can provide analytical precision of the order of ±0.15 μmol mol^{-1} for CO_2, ±0.9 nmol mol^{-1} for CH_4, ±0.3 nmol mol^{-1} for N_2O, and ±0.3 nmol mol^{-1} for CO, expressed as mole fractions in dry air. The analytical precision is in all cases competitive with or superior to that of the more usual methods of analysis for these trace gases, namely, nondispersive infrared spectroscopy for CO_2 and gas chromatography-based techniques for CH_4, N_2O, and CO. The novel FT-IR method relies on calibration using synthetically calculated absorbance spectra and a chemometric multivariate calibration algorithm, classical least squares.

The three most important anthropogenically influenced greenhouse gases are carbon dioxide, methane, and nitrous oxide.[1] While not directly a greenhouse gas, carbon monoxide also plays an important role in atmospheric chemistry as one of the most important factors determining the concentration of atmospheric oxidants.[2] Measurements of the spatial distribution and temporal trends of these species in the atmosphere have played, and will continue to play, a key role in the elucidation of their atmospheric budgets. New measurement technologies have the potential to offer improvements over current strategies, as well as providing a means of independently asessing well-established technologies.

There is a high degree of consensus on the choice of instrumental techniques employed for point sampling in situ measurement of atmospheric trace gases. The nondispersive infrared (NDIR) spectroscopy method described by, for example, Komhyr et al.[3] still predominates[4] for background atmospheric CO_2 monitoring. This method offers a short-term precision (one standard deviation) as good as ±0.01 in 360 μmol mol^{-1} (mole fraction mixing ratio) or ±0.003%, for an hourly mean measurement. Alternatively, CO_2 can be separated by gas chromatography (GC), converted to methane over a catalyst, and detected with a flame ionization detector (FID). This GC-methanizer-FID approach can offer a short-term precision level of ±0.02%.[5] The other three gases mentioned are usually analyzed using gas chromatography. Methane in air lends itself readily to analysis by GC-FID as described by Steele et al.,[6] where a precision level of ±2.5 nmol mol^{-1} in atmospheric background levels of 1720 nmol mol^{-1} CH_4, or ±0.15%, is attainable.[5,7] For N_2O in air, GC with electron capture detection (ECD) remains the standard technique. Precision of the order of ±0.3 in 300 nmol mol^{-1} N_2O, or ±0.1%, is attainable.[5,8] Analysis of CO at background atmospheric levels is usually done by GC separation followed by the reduction of hot HgO to Hg by CO, the Hg vapor being measured by UV absorption.[5,9,10] This ensemble is known as a mercuric oxide reduction gas detector (RGD). Precision of ∼±1% can be obtained at 100 nmol mol^{-1} CO.

Using the orthodox analytical techniques just described to measure or routinely monitor the four species CO_2, CH_4, N_2O, and CO, simultaneously at a single site currently requires an ensemble of four separate instruments: NDIR (or GC-methanizer-

* Corresponding author: (e-mail) mesler@uow.edu.au. (fax) +61-2-4221-4287.
† University of Wollongong.
‡ CSIRO Atmospheric Research.

(1) Schimel, D.; Alves, D.; Enting, I.; Heimann, M.; Joos, F.; Rayneud, D.; Wigley, T.; Prather, M.; Derwent, R.; Ehhalt, D.; Fraser, P.; Sanhueza, E.; Zhou, X.; Jonas, P.; Charlson, R.; Rodhe, H.; Sadasivan, S.; Shine, K. P.; Fouquart, Y.; Ramaswamy, V.; Solomon, S.; Srinivasan, J.; Albritton, D.; Derwent, R.; Isaksen, I.; Wuebbles, D. In *Climate Change 1995*: *The Science of Climate Change* (*Intergovernmental Panel on Climate Change*); Haughton, J. T., Meira Filho, L. G., Callander, B. A., Harris, N., Kattenberg, A., Maskell, K., Eds.; Cambridge University Press: Cambridge, 1996; pp 65−131.
(2) Thompson, A. M. *Science* **1992**, *256*, 1157−1165.
(3) Komhyr, W. D.; Harris, T. B.; Waterman, L. S.; Chin, J. F. S.; Thoning, K. W. *J. Geophys. Res.* **1989**, *94*, 8533−8547.
(4) Steele, L. P.; Beardsmore, D. J.; Pearman, G. I.; Da Costa, G. A. In *Baseline Atmospheric Program Australia 1994−95*; Francey, R. J., Dick, A. L., Derek, N., Eds.; Bureau of Meteorology and CSIRO Division of Atmospheric Research: Melbourne, 1996; p 103.
(5) Francey, R. J.; Steele, L. P.; Langenfelds, R. L.; Lucarelli, M. P.; Allison, C. E.; Beardsmore, D. J.; Coram, S. A.; Derek, N.; de Silva, F. R.; Etheridge, D. M.; Fraser, P. J.; Henry, R. J.; Turner, B.; Welch, E. D.; Spencer, D. A.; Cooper, L. N. In *Baseline Atmospheric Program* (*Australia*) *1993*; Francey, R. J., Dick, A. L., Derek, N., Eds.; Bureau of Meterology and CSIRO Division of Atmospheric Research: Melbourne, 1996; pp 8−29.
(6) Steele, L. P.; Fraser, P. J.; Rasmussen, R. A.; Khalil, M. A. K.; Conway, T. J.; Crawford, A. J.; Gammon, R. H.; Masarie, K. A.; Thoning, K. W. *J. Atmos. Chem*. **1987**, *5*, 125−171.
(7) Dlugokencky, E. J.; Steele, L. P.; Lang, P. M.; Masarie, K. A. *J. Geophys. Res.* **1995**, *100*, 23103−23113.
(8) Prinn, R.; Cunnold, D.; Rasmussen, R.; Simmonds, P.; Alyea, F.; Crawford, A.; Fraser, P.; Rosen, R. *J. Geophys. Res.* **1990**, *95*, 18369−18385.
(9) Crill, P. M.; Butler, J. H.; Cooper, D. J.; Novelli, P. C. In *Biogenic Trace Gases*: *Measuring Emissions from Soil and Water*; Matson, P.A., Harriss, R. C., Eds.; Blackwell: Oxford, 1995; pp 164−205.
(10) Novelli, P. C.; Elkins, J. W.; Steele, L. P. *J. Geophys. Res.* **1991**, *96*, 13109−13121.

10.1021/ac9905625 CCC: $19.00
Published on Web 11/30/1999

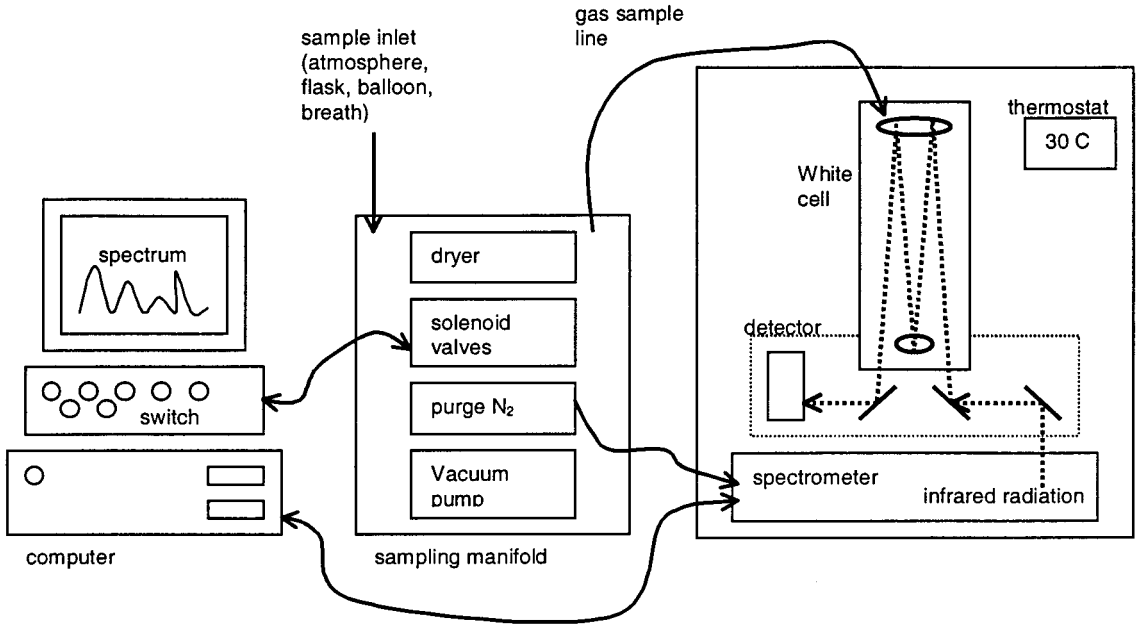

Figure 1. Simple schematic of the instrument.

FID), GC-FID, GC-ECD, and GC-RGD. In turn, it is necessary to characterize four separate instrument response functions and implement four calibration protocols. We describe here a single FT-IR spectrometer configured to provide the same analyses, simultaneously and with the same level of precision. In the following paper, we describe the application of FT-IR spectroscopy to the determination of the stable isotope ratio $^{13}C/^{12}C$ in atmospheric CO_2.[11]

EXPERIMENTAL SECTION

The configuration of the instrument used in this work is illustrated schematically in Figure 1. Briefly, a commercially available Bomem MB100 FT-IR spectrometer, with 1-cm^{-1} maximum resolution, globar source, KBr beam splitter, and a liquid nitrogen-cooled InSb infrared detector, was used to analyze air samples introduced to a multipass (White) cell. The instrument and White cell were enclosed in a sealed, thermostated box which was purged with dry nitrogen.

This section also considers the main experimental factors in obtaining good-quality spectra: namely, spectrum signal-to-noise ratio, detector linearity, Beer−Lambert law linearity, temperature and pressure control, instrument environment and sample processing.

Spectrum Signal-to-Noise Ratio. Spectra were collected at the spectrometer's maximum resolution, 1 cm^{-1}. Of the four molecular species of interest in this work, some of the rotational structure of three of them is resolved at this resolution in the 2000−3000-cm^{-1} region, as illustrated in Figure 2. The rotational transitions are separated by less than 1 cm^{-1} and remain unresolved only for N_2O. (The approximate rotational separations in the most intense absorption features are as follows: CO_2 ~1.6 cm^{-1}, CH_4 ~9.0 cm^{-1}, CO ~3.8 cm^{-1}, and N_2O ~0.8 cm^{-1}). For the three less abundant trace gases, CH_4, CO, and N_2O, with the correspondingly weak absorption features, signal-to-noise ratio

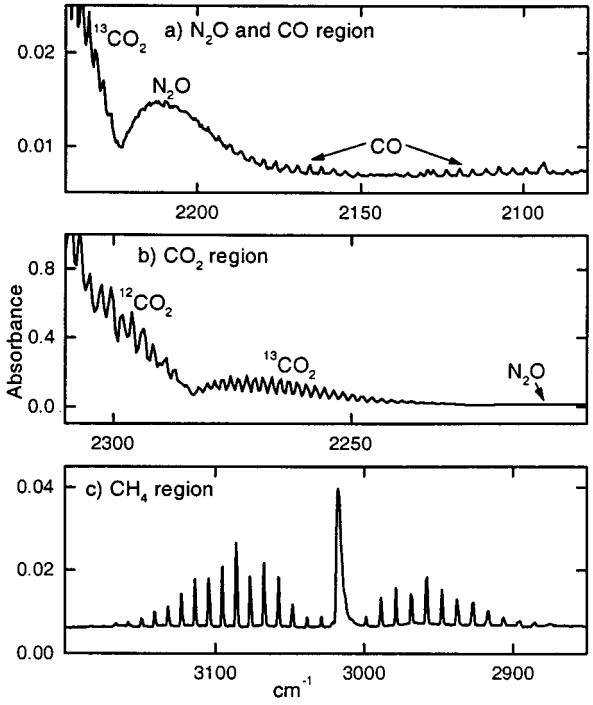

Figure 2. Regions of an infrared absorbance spectrum of air showing (a) $^{13}CO_2$, N_2O, and CO; (b) $^{12}CO_2$, $^{13}CO_2$, and N_2O; and (c) CH_4 absorbance features.

(SNR) was the limiting factor on the analytical precision achieved, while for CO_2 it was departure from Beer−Lambert law linearity.

The White cell serves to increase the absorbance relative to noise in the absorbance spectrum by increasing the path length without proportional loss of signal.[12−14] Two different White cells were used as described in Table 1. Although the 22-m cell provides the best result in terms of absorbance relative to noise, consideration of the scarcity and expense of calibration gases will favor

(11) Esler, M. B.; Griffith, D. W. T.; Wilson, S. R.; Steele, L. P. *Anal. Chem.* **1999**, *71*, 216−221 (this issue).

(12) White, J. U. *J. Opt. Soc. Am.* **1942**, *32*, 285−288.
(13) White, J. U., *J. Opt. Soc. Am.* **1976**, *66*, 411−416.
(14) Horn, D.; Pimentel, G. C. *Appl. Opt.* **1971**, *10*, 1892−1898.

Table 1. Specifications of the Two Multipass White Cells Used

	22 m cell	9.8 m cell
base path length, m	1.1	0.25
total path length, m	22.1	9.8
no. of passes	20	40
volume, L	8	0.5
transmitted energy, %	~20	~12

the smaller volume 9.8-m cell for many applications, particularly for CO_2 analysis where precision is not limited predominantly by SNR. This cell has the added advantages of being quicker to fill and pump out and, being smaller, is more easily incorporated in a field-deployable instrument than the 22-m cell.

Detector Noise and Linearity. Detector noise was minimized with the use of a liquid nitrogen-cooled InSb detector, which had a specific peak detectivity (D^*) of 1.9×10^{11} cm $Hz^{1/2}$ W^{-1} and is ideally suited to the 2000−3000-cm^{-1} region of the spectrum where CO_2, CH_4, CO, and N_2O have strong absorbance features. A bandpass filter (OCLI, serial number W03999-4) to select only the region containing the main CO_2, CH_4, CO, and N_2O transitions, i.e., 2000−3200 cm^{-1}, was used to avoid detector saturation.

There is a tradeoff between spectrum averaging time and SNR (see Griffiths and de Haseth[15] for a full account of the trading rules in FT-IR spectroscopy). To double the SNR, the averaging time (or the number of coadded scans, in effect) must be quadrupled. For averaging times of up to ~8 min (~256 scans), the quality of the spectral fit (and hence the precision of the technique as measured by SEP) appears to be limited by high-frequency noise. This high-frequency noise is reduced by extending the coaddition time. Low-frequency effects such as drifts in baseline are well modeled by our classical least-squares (CLS) approach within this domain. However, beyond ~8 min, the quality of the spectral fit appears to be limited by features in the spectrum that are not so well modeled by the CLS calibration such as more complex features in the baseline or residual line shape effects. So coadding for longer than 8 min brings no further gains in precision. In any case, an 8-min or less measurement is practical for many applications. When the SNR-sensitive CO, CH_4, and N_2O were the subject of analysis, ~256 scans, or 8 min, was found to be optimal. This was sufficient to provide single-beam root-mean-squared (rms) SNR of ~50 000; equivalently absorbance spectra with rms noise levels of the order of 10^{-5} at 2000 cm^{-1}. The experimentally determined relationship between precision and averaging time is illustrated in the section on verification of the method, below.

Beer−Lambert Law, Linearity, Apodization, and Resolution. The Beer−Lambert law may be stated as $A = \alpha cl$, where A is absorbance, α is absorption coefficient, c is concentration, and l is path length. In FT-IR spectroscopy, there will be a deviation from Beer−Lambert law behavior where the absorption features are narrower than can be resolved using the available instrumental resolution. Zhu and Griffiths[16] have quantified the expected deviations from Beer−Lambert linearity for triangular and other

(15) Griffiths, P. R.; de Haseth, J. A. *Fourier transform infrared spectrometry*; John Wiley and Sons: New York, 1986.
(16) Zhu, C.; Griffiths, P. R. *Appl. Spectrosc.* **1998**, *52*, 1403−1408.

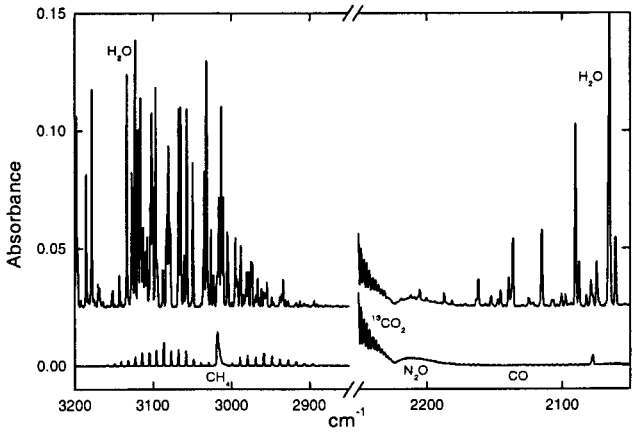

Figure 3. Absorbance spectra of wet (top) and dried (bottom) air, at 740 Torr and 305 K. The wet air contains ~1% H_2O, and the dried air contains <10 μmol mol^{-1} H_2O.

apodization functions across a range of possible experimental configurations. Below a certain threshold, absorbance will vary linearly with concentration. In the earlier stages of our work, all interferograms were processed using a triangular apodizing function. Later, a Happ−Genzel apodizing function was employed. The latter allowed improved analytical precision as well as extending the range of absorbances for which Beer−Lambert law linearity prevailed. In our instrumental configuration, we have found that the strength of the peak absorbance features due to CO, N_2O, CH_4, and $^{13}CO_2$ were well within this region of Beer−Lambert linearity. Some of the $^{12}CO_2$ lines used for analysis were somewhat stronger and potentially nonlinear. However, we have found experimentally that the degree of nonlinearity was not a source of systematic error for measured peak absorbances up to ~0.4. Thus, regions of the spectrum with absorbance greater than 0.4 are not used in the calibration and quantitative analysis strategies described below.

Temperature and Pressure Control. Spectroscopy inherently measures concentration (mass or mole per volume) for a constant path length. To convert concentration to mixing ratio requires the measurement of the sample density, achieved by measuring temperature and pressure. The sample pressure was determined with a capacitance manometer mounted on the White cell. The temperature was measured with platinum resistance temperature detectors (RTDs). The manometer and RTD output was monitored with a 16-bit data acquisition card. Sample pressure was typically in the range 720−760 Torr. The precision of the pressure measurement in this range was of the order of ±0.1 Torr, or ±0.01% at 760 Torr. The precision of the RTDs was better than ±0.03 K, or ±0.01% in 300 K. The pressure and temperature measurements should not, therefore, limit the precision of the method.

Instrument Environment. The spectrometer and White cell were enclosed in a thermostated box and purged with dried high-purity N_2 at a rate of 500−1000 mL min^{-1}. Purging removes absorbing species from the part of the optical path lying outside the White cell. Thermostating was required to minimize instrument drift which otherwise becomes limiting to final measurement precision.

Sample Processing. Figure 3 illustrates the difference between the spectra of ambient air, dew point ~7 °C, containing

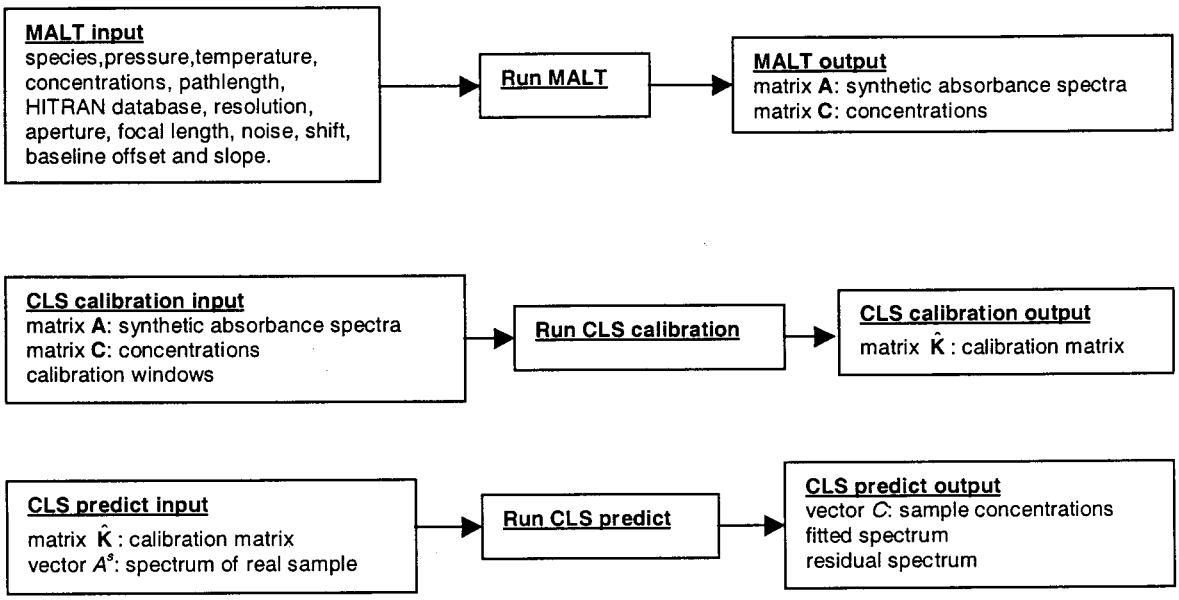

Figure 4. Flow chart of calibration and prediction process using MALT and CLS.

~1% H_2O, and dried air. Strong H_2O absorption features occur in the same region as CH_4, N_2O, and CO. In principle, the quantitative spectrum analysis algorithm employed (described below) is capable of resolving individual species contributions to a spectrum of their mixture, even when the absorption lines obscure and overlap each other seriously, as in Figure 3. In practice, significantly greater reproducibility is obtained for CH_4, N_2O, and CO mixing ratio retrievals if the samples are well dried first. The H_2O absorption lines, as well as obscuring the usually much weaker CH_4, N_2O, and CO features, are sufficiently strong to behave in a nonlinear Beer−Lambert manner. This can introduce serious "analytical cross-talk" into the fitting procedure, where the apparent mixing ratios of CH_4, N_2O, and CO will be slightly dependent on the level of H_2O present. In ambient air, moisture levels are typically in the range 0.5−2.5% and are quite variable with time. Accordingly, all samples were dried to $<10\ \mu$mol mol^{-1} H_2O (−70 °C dew point) prior to analysis by passing them over anhydrous magnesium perchlorate, a very efficient desiccant. A stainless steel cartridge, volume ~200 mL, was filled with granulated anhydrous magnesium perchlorate and placed in the sampling line. Sample residence time in the dryer is <1 s. One such charge of desiccant was sufficient to dry ~1600 L of ambient air. This desiccant is known not to perturb the concentrations of CO_2, CH_4, N_2O, and CO in air.[5]

As far as possible, the sampling manifold was constructed of glass, copper, and stainless steel tubing, PTFE (Teflon), and Viton. The system was kept as free as possible of hydrocarbons. The moving components in the solenoid valves were cleaned of lubricants. An activated alumina hydrocarbon trap was fitted to the rotary oil pump to prevent backstreaming of oil vapors to the manifold and White cell.

The random error in the analysis due to the inconsistency of the human operator was effectively removed by automation. A program in the GRAMS-Array Basic (Galactic Industries Inc.) language was used to automate the FT-IR analysis. The program addressed a data acquisition and control card (Strawberry Tree Industries, Mini-16) to activate the solenoid valves for sample handling and to log temperature and pressure. A 16-bit ADC was used to ensure that measurement precision was not limited by the ADC. In each cycle of the program, single-beam spectra were collected, saved to disk, and ratioed with reference spectra to produce absorbance spectra which were then fitted as described in the quantitative analysis section below. The parameters of the fit provided the concentration of the trace gas constituents directly. These are combined with pressure and temperature data to provide mixing ratios.

QUANTITATIVE ANALYSIS OF SPECTRUM

This section deals only with how the absorbance spectra of air samples were analyzed. This may be considered as a three-phase process, as outlined in Figure 4. In the first phase, the multiple atmospheric layer transmission (MALT) program[17] is used to calculate a set of absorbance spectra, **A**, that closely simulate the spectra obtained on the actual instrument. In the second phase, this set of spectra, **A**, and a matrix, **C**, containing the trace gas concentration information for the calculated spectra are used as the training set input to the multivariate calibration algorithm, in this case CLS.[18] In practice, the entire calculated spectrum is not used for calibration. Rather, an optimized region within the spectrum is chosen for each species. A procedure for optimal spectral region selection is detailed below. In the second phase, the CLS calibration algorithm produces as its output a matrix, $\hat{\mathbf{K}}$, the calibration matrix, which describes the relationship between species concentration and absorbance strength for all species and regions of the spectrum included in the calibration. Absorbance is assumed to be proportional to concentration (Beer−Lambert law) at all wavenumbers $\tilde{\nu}$. The third phase is the prediction CLS step, in a sense the inverse of the calibration CLS step. The calibration matrix, $\hat{\mathbf{K}}$, is used to perform a linear least-squares fit of a synthetic spectrum to a real experimental spectrum, A^s. The parameters of the fit, the vector C, directly give

(17) Griffith, D. W. T. *Appl. Spectrosc.* **1996**, *50*, 59−70.
(18) Haaland, D. M.; Easterling, R. G.; Vopicka, D. A. *Appl. Spectrosc.* **1985**, *39*, 73−84.

the concentrations of the trace gas components of the real sample.

Müller et al.[19] have recently shown the effects of wavenumber scale instability on FT-IR trace gas measurements when using a multivariate analysis approach in the absorbance domain. To avoid these effects, we iteratively fit the wavenumber scale simultaneous to the CLS process of fitting the absorbance scale. This is done rapidly in real time by computer and means that any wavenumber instability will not affect the fitting of spectral absorbances and hence the retrieved component concentrations.

Normally, the first step, MALT simulation, and the second step, CLS calibration, need to be performed once for a given type of analysis. The resulting calibration matrix $\hat{\mathbf{K}}$ is stored in the computer. The CLS prediction step is performed every time a spectrum is fitted to derive its concentrations. The first and second steps can be completed in a few minutes. The third step takes less than 1 s of computer time and so may be performed on-line in real time following the collection of each spectrum.

CLS−Multivariate Calibration and Prediction. CLS analysis is one of several chemometric techniques developed in the past decade or so and is ideally suited to the retrieval of quantitative information from spectra. The theory is fully described elsewhere.[18] We used a CLS package originating from Galactic Industries Inc. which has been significantly customized for this application.

A general disadvantage of the CLS method is that all interfering chemical components in the spectral region of interest need to be known and included in the calibration or the method will give erroneous results. In many analytical situations, this renders CLS an inappropriate chemometric technique. Often, the conceptually similar but more complex partial least-squares (PLS) technique is applied. The significant advantage of PLS over CLS is that PLS does not require that all absorbing components of the system be known, as long as the variance of the training set adequately represents the variance of the unknown spectra. The disadvantage of PLS is that much of the transparency of CLS and the valuable qualitative information it provides is lost. Indeed, Haaland et al.[20] have recently described the use of CLS to shed light on PLS calibrations of solution spectra. In the present work all significant absorbing components of the sample are known; they are H_2O, CO_2, CO, and N_2O in the 2000−2500-cm^{-1} region and CH_4 near 3000 cm^{-1}. Except for rare contamination events due to nonmethane hydrocarbons, the absorbance due to other trace gas species is less than the noise level of the recorded spectra. This enables the system to be fully characterized, i.e., calibrated in all absorbing species present, as required when the CLS technique is employed. In the developmental stage of this project, a parallel study was performed, where both CLS and PLS techniques were applied to analysis of the same samples. The results indicated that there was nothing to be gained by using PLS rather than the simpler CLS. While it was observed that PLS typically gave better fits to experimental spectra than did CLS, this did not translate into higher analytical precision for trace gas analysis.

MALT/HITRAN (Working Calibration). MALT, a program for generating synthetic absorbance spectra, has been described fully elsewhere.[17] Normally real experimental spectra are required as calibration input to the CLS calibration algorithm. For the simultaneous analysis of several atmospheric trace gas species in air, these calibration spectra would be obtained by analyzing a suite of air samples of known composition. Furthermore, within this suite it would be necessary to ensure that the concentration of the different species varied independently from each other and covered the range of concentrations anticipated in any unknown samples to be analyzed. MALT removes the need for a suite of real calibration gases since it calculates simulated spectra which model very closely the real spectra obtained using a given FT-IR spectrometer. A change in measurement conditions merely requires the rerunning of MALT to update the calibration. What follows is only a brief summary of MALT.

The calculation of synthetic spectra is based on a compilation of absorption line parameters. One suitable line parameter set is HITRAN,[21] which includes line parameters for 35 individual atmospheric gases, including the species of interest here. HITRAN includes, for each absorption line of each molecule, the line frequency, the integrated line strength, and the pressure and temperature-dependent Lorentzian half-width. For each absorption line of each molecule, MALT first calculates the contribution to the absorption coefficient at each wavenumber. This includes temperature and pressure contributions to the strengths and line shape due to both Doppler and pressure broadening. The absorption coefficient is then multiplied by the amount of the molecular species (i.e., its concentration times the path length) to provide the monochromatic optical depth, τ, at any given wavenumber. The total monochromatic optical depth spectrum is arrived at by summing over all absorption lines of all molecules. This spectrum is equivalently the spectrum measured on a perfect spectrometer of arbitrarily high resolution. However, any real spectrometer convolves the true monochromatic transmission (transmission $= e^{-\tau}$) spectrum with an instrument line shape to produce the observed or measured transmission spectrum. MALT models the contributions to instrument line shape due to instrument resolution (finite optical path difference), the apodization function applied to the interferogram, and to the divergence of the collimated beam in the spectrometer. When these effects are convolved with the monochromatic transmission spectrum, the result is the instrumentally degraded spectrum. MALT converts this into the required output units (for either transmittance or absorbance), and it is saved in the standard GRAMS (Galactic Industries) file format.

For a set of calibration spectra, the number of spectra required and the range of concentrations for each absorber are input to MALT and a set of spectra with random concentrations within the given ranges is calculated. Random noise may also be optionally included in MALT calculated spectra. Finally, the calibration set calculation also produces a list file of all calibration spectra and their species concentrations in a format suitable to define the **C** matrix for direct input to the CLS software.

In operational terms, one full run of MALT is equivalent to the generation of a full set of calibration spectra. Typically 40

(19) Müller, U.; Heise, H. M.; Mosebach, H.; Gärtner, A. G.; Hausier, T. *Field Anal. Chem. Technol.* **1999**, *3*, 141−159.

(20) Haaland, D. M.; Han, L.; Niemczyk, T. M. *Appl. Spectrosc.* **1999**, *53*, 390−395.

(21) Rothman, L. S.; Rinsland, C. P.; Goldman, A.; Massie, S. T.; Edwards, D. P.; Flaud, J.-M.; Perrin, A.; Camy-Peyret, C.; Dana, V.; Mandin, J.-Y.; Schroeder, J.; McCann, A.; Gamache, R. R.; Wattson, R. B.; Yoshino, K.; Chance, K. V.; Jucks, K. W.; Brown, L. R.; Nemtchinov, V.; Varanasi, P. *J. Quant. Spectrosc. Radiat. Transfer* **1998**, *60* (*5*), 665−710.

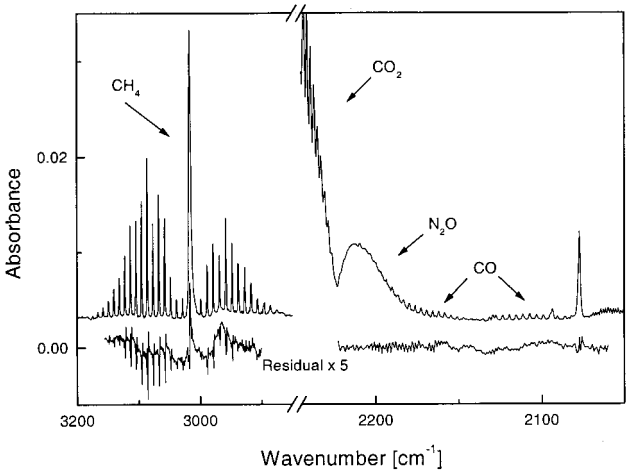

Figure 5. Example of two regions of a real spectrum of clean air, and the residual spectrum (difference between real and fitted spectra, enlarged ×5) resulting from the CLS fit of MALT/HITRAN calculated spectra to the real spectrum. The sharp features evident in the CH_4 residual spectrum are most likely due to inadequate MALT modeling of the actual instrumental line shape which may be asymmetric due to misalignment and pressure shifts.

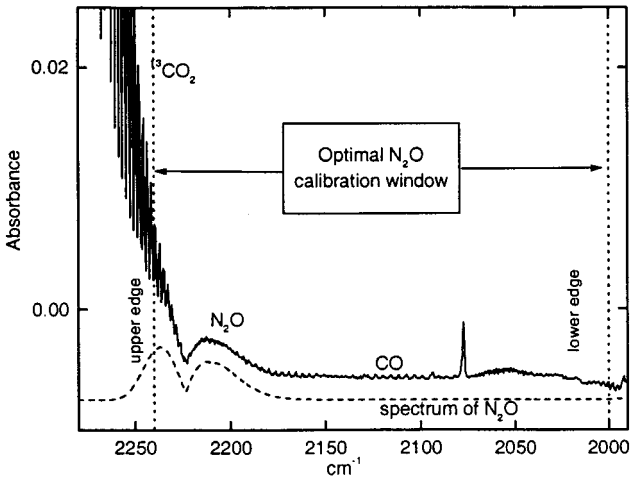

Figure 6. Spectrum of air sample and of the N_2O component of the air, showing the optimal spectroscopic window for N_2O analysis.

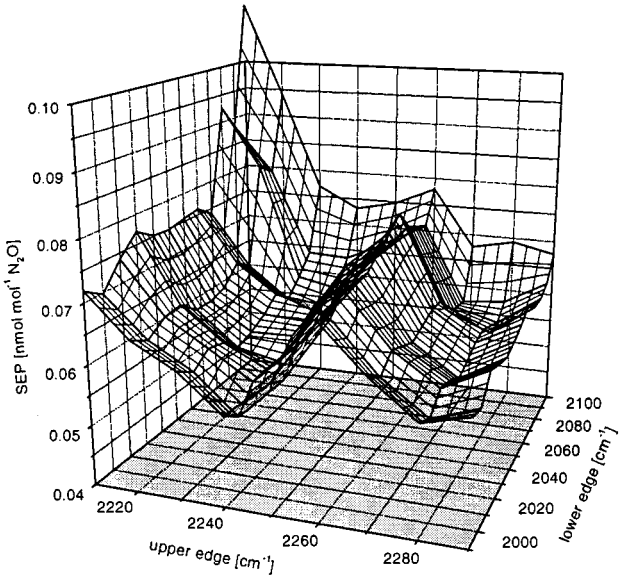

Figure 7. MALT-modeled SEP surface for N_2O. SEP of calibration vs upper and lower edge of spectrum region used in calibration.

spectra were calculated. The number of calibration spectra required depends in part on deviations from the ideal Beer−Lambert law; in an ideal Beer−Lambert case, if there are *N* components and no noise, only *N* spectra are required. However, as the spectra are generated synthetically on a computer within reasonable time limits, the cost in time of generating large calibration sets is negligible. There is no advantage in generating fewer spectra. When fitting real spectra with MALT/CLS-calculated synthetic spectra, it is possible to achieve very good fits where the residual spectrum (difference between the fitted and the real spectra) is dominated by the random spectral noise. For example, Figure 5 illustrates an example of the CLS best fit to two regions of a real spectrum, based on a set of calibration spectra calculated by MALT/HITRAN. The real spectrum is that associated with a clean air sample. The residual spectrum is useful as a diagnostic indicator of the quality of the fit. In this case, random noise dominates the CO and N_2O region of the residual spectrum indicating a good fit, but the CH_4 residual spectrum shows evidence of an imperfect MALT modeling of the CH_4 line shape.

Absolute Calibration. The process just described, of using the MALT-calculated spectra derived from the HITRAN database and CLS analysis serves to carry out a working, or "MALT/CLS", calibration of the instrument. This is sufficient to determine the analytical precision of the method, for example, as illustrated in Figure 8. However if we wish to probe the accuracy of the method, this MALT/CLS calibration must be referenced to an independent "absolute" scale. An "absolute" calibration of the FT-IR instrument can be carried out by analyzing real samples from a suite of calibration tanks containing air that has been independently calibrated relative to reference standards and then determining their apparent composition using the MALT/CLS calibration. Absolute calibration allows for the effects of uncertainty in path length, instrumental line shape, and HITRAN line parameters to be largely removed from the measurement. We have carried out a study (which will be reported fully elsewhere) in which a suite of 24 reference air tanks was analyzed by FT-IR. Each tank had independently been assigned mixing ratios for one or all of the species CO_2, CH_4, CO, and N_2O by GASLAB (Global Atmospheric Sampling LABoratory, CSIRO Atmospheric Research, Australia). The links between the GASLAB scales and existing calibration scales that are internationally recognized are described in Francey et al.[5] The trace gas mixing ratios in the set of tanks more than spanned the range of mixing ratios typically found in the atmosphere. For all four species, we found that the MALT/CLS calibration was linearly related to the GASLAB scale over the entire range of mixing ratios tested, but that there can be a systematic difference of up to 5% between the MALT/CLS-derived mixing ratios and those on the GASLAB scales. We have found that in practice reference to one or two air standards is sufficient to relate the MALT/CLS calibration to some absolute scale to a high degree of accuracy. For example, Figure 9 (discussed below) illustrates five weeks of half-hourly FT-IR trace gas monitoring data which are accurate (i.e., in agreement with parallel measurements using conventional instruments) to the order of 0.1% for CO_2, CH_4, N_2O, and 1% for CO.

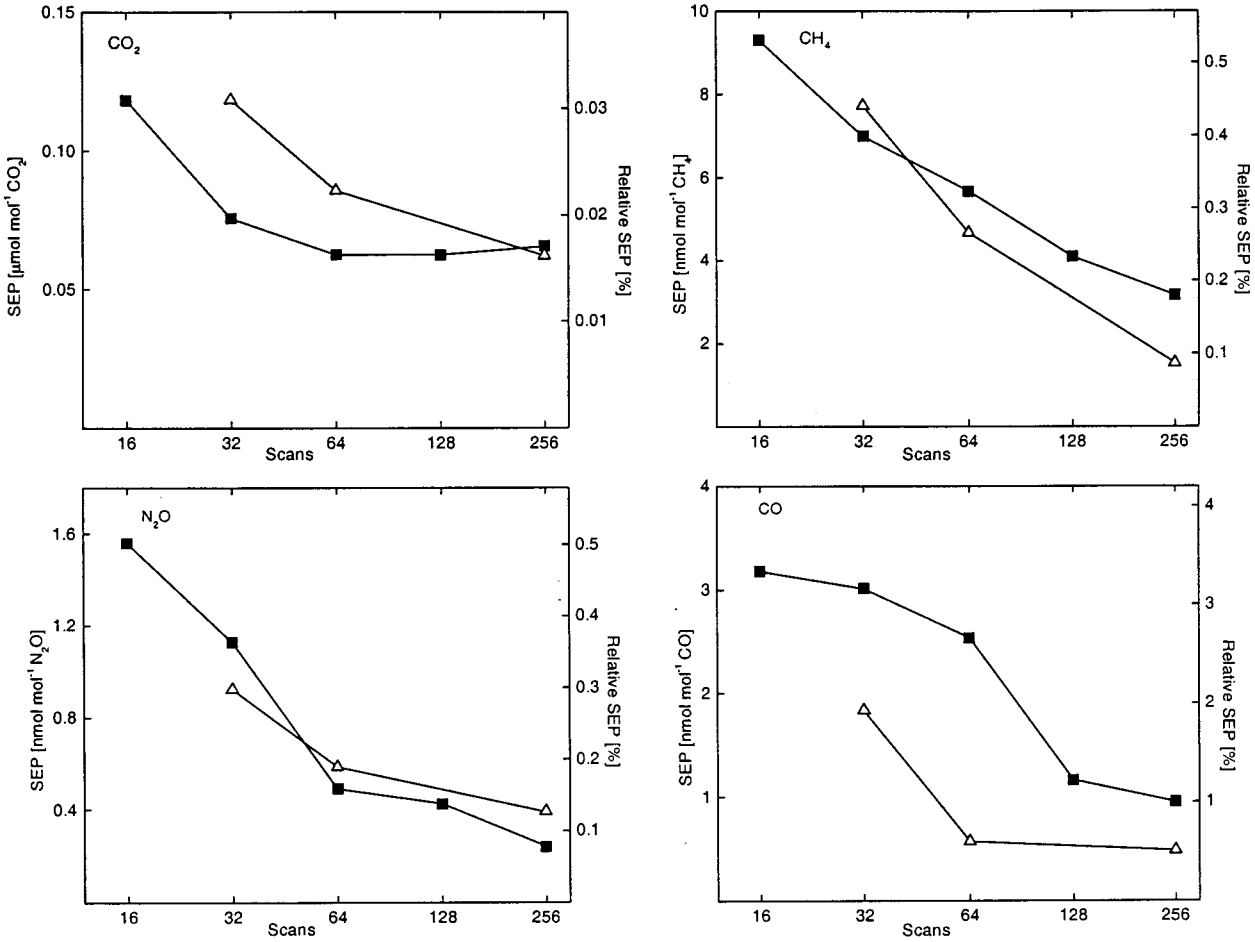

Figure 8. Experimental SEP vs number of coadded scans for CO_2, CH_4, N_2O, and CO. Filled squares indicates the no-sample-handling experiment results, and open triangles are the spectroscopy + sample handling results. (MALT parameters: resolution 1 cm^{-1}, 740 Torr, 305 K, path length 9.8 m, 0 < H_2O < 10 μmol mol^{-1}, 340 < CO_2 < 380 μmol mol^{-1}, 1680 < CH_4 < 1750 nmol mol^{-1}, 300 < N_2O < 320 nmol mol^{-1}, and 50 < CO < 100 nmol mol^{-1}. CLS calibration windows: $^{12}CO_2$ 2020−2306 cm^{-1}; $^{13}CO_2$ 2020−2290 cm^{-1}; CH_4 2805−3195 cm^{-1}; CO 2020−2200 cm^{-1}; N_2O 2020−2250 cm^{-1}.)

Optimal Spectral Window Selection. It is necessary to decide which region(s) of the spectrum to fit for the analysis of each species. For example, Figure 6 illustrates a spectrum of a sample of air that includes 310 nmol mol^{-1} N_2O. The calculated spectrum for N_2O is also illustrated, offset in the *y*-axis for clarity. Virtually all the infrared absorption features for the species N_2O occur in the region 2160−2260 cm^{-1}, suggesting this as an appropriate calibration window. However, there are significant gains to be made in precision by systematically rather than intuitively determining the ideal upper and lower edges of the calibration window for each species. Note that for N_2O in air the P-branch (2160−2225 cm^{-1}) lies relatively clear of other absorption bands with just a few weak CO line overlapping with it. The R-branch (2225−2260 cm^{-1}) lies under considerably stronger absorption lines due mainly to $^{13}CO_2$. If a decision is made to fit N_2O only in the region not obscured by $^{13}CO_2$, then this may effectively discard as much as half of the N_2O information which could potentially have made the measurement more precise. If, on the other hand, all of the N_2O information under $^{13}CO_2$ is included, the risk of having the N_2O measurement perturbed by interference from the much stronger $^{13}CO_2$ absorption features is much higher.

For ideal spectra, the optimal CLS window for a species can be systematically determined solely by use of MALT-calculated spectra and the CLS calibration procedure. The first step is to generate a set of spectra using MALT that closely simulates the line shape and range of concentrations of the instrumentally obtained spectra to be analyzed, including realistic levels of noise. The wavenumber region of the MALT spectra should extend beyond the range of wavenumber regions to be considered for the optimal calibration window. First a guess at the best left and right edges of the calibration window is made. Using these, along with the MALT-calculated spectra as input, the CLS calibration step is undertaken. As well as producing a calibration, the CLS algorithm produces as output a statistical estimate of the precision of that calibration. This is the standard error of prediction (SEP) of the calibration:

$$\mathrm{SEP} = \sqrt{\frac{\sum_n (y_{\mathrm{actual}} - y_{\mathrm{predicted}})^2}{n}}$$

There are n (typically 40) spectra in the calibration training set, and y_{actual} and $y_{\mathrm{predicted}}$ are the actual and CLS-predicted concentrations, respectively, of a given species in a particular training spectrum. In the calculation of the SEP, each spectrum in turn is

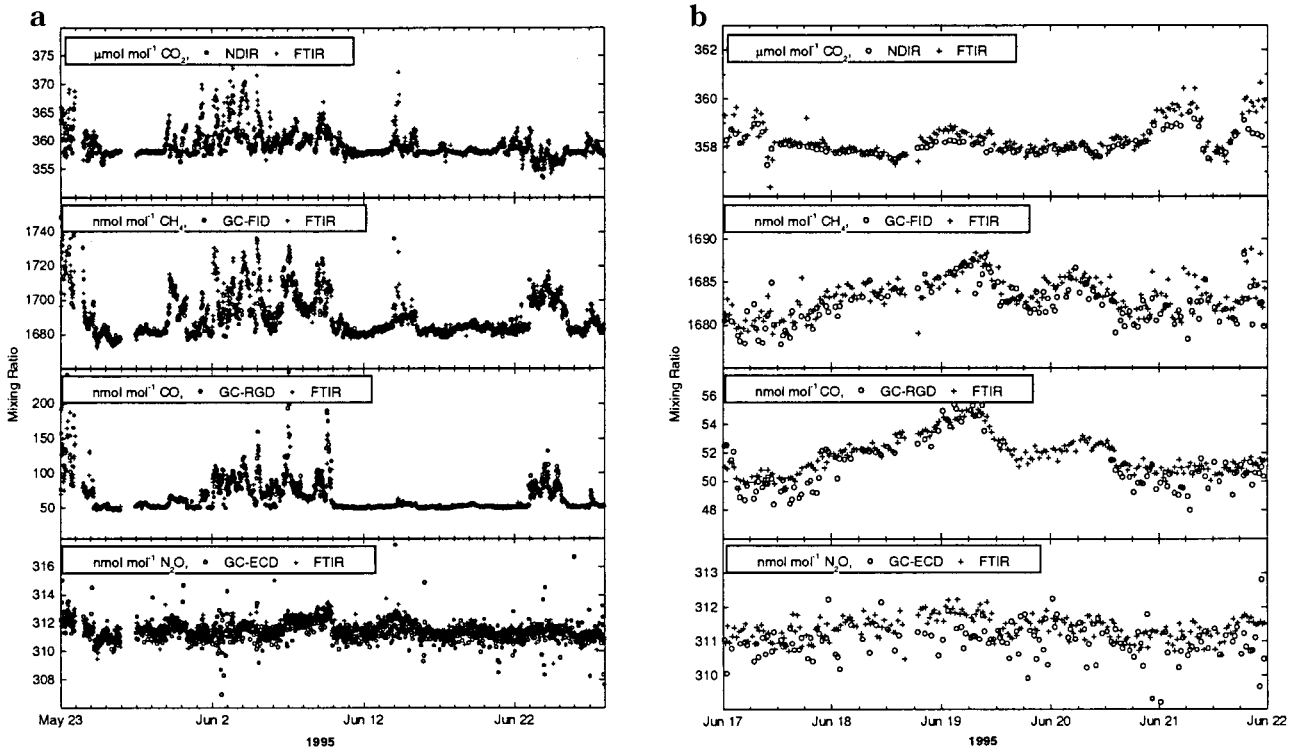

Figure 9. FT-IR, AGAGE-GC, and NDIR trace gas mixing ratios at Cape Grim (a) during the period 23 May−28 June, 1995 and (b) during an extended period of clean air conditions, June 17−22, 1995.

removed from the calibration set and is predicted by the n - 1 others, to avoid self-prediction.

For a given set of input spectra and a given calibration window specified by its upper and lower edges, the CLS calibration step estimates how precisely it can retrieve each species concentration from the spectroscopic information provided in that window. To systematically determine the optimal window for a given species, the CLS calibration step is performed many times while the calibration window is systematically varied. The minimum SEP specifies the calibration window that will produce most precise retrievals of that species concentration from MALT spectra. The assumption is then made that the same SEP vs window edge surface will give a good indication of achievable precision for real as opposed to synthetic spectra.

Figure 7 illustrates such an SEP surface for calibration of N_2O measurements in the region of the spectrum bounded by 1990 and 2290 cm^{-1}. The lower limit of the lower edge was determined by the cutoff of the optical filter we used. The position of the minimum on this surface suggests that an optimal choice for an N_2O calibration window would be the region 2000−2240 cm^{-1}. This optimal window is illustrated in Figure 6. Choosing an upper edge much higher than 2240 cm^{-1} leads to a loss of measurement precision due to the inclusion in the window of too much strong $^{13}CO_2$ information which obscures or dilutes the N_2O information content. Somewhat counterintuitively, the optimal lower edge for the N_2O window is 2000 cm^{-1}, resulting in the inclusion of a large region where there is very little absorption, by N_2O or any other species, other than the sharp CO_2 feature at 2075 cm^{-1}. It is plausible that the inclusion of this CO_2 feature in the calibration window helps to constrain N_2O. However, on the basis of observations of the other species' optimal calibration windows, we believe the main beneficial effect is due to the inclusion of the baseline regions. Only when the baseline is well characterized are the nonbaseline absorption features well constrained by reference to it, thus leading to improved measurement precision. This is particularly important for a broad "featureless" spectrum such as N_2O. Similar precision surfaces for the molecules CO_2, CH_4, and CO are generated in the same way.

VERIFICATION OF METHOD AND APPLICATION TO ATMOSPHERIC MONITORING

A series of instrumental and modeling experiments was performed in an attempt to verify the validity of the approach described above. We also report results of a field trial of the instrument where it was employed to continuously monitor trace gases.

Experimental Precision. A sample of air was introduced to the 9.8-m path length White cell from a calibration tank. This air was known from independent gas chromatographic analysis by GASLAB to have the following approximate trace gas mixing ratios: 358 μmol mol^{-1} CO_2, 1700 nmol mol^{-1} CH_4, 90 nmol mol^{-1} CO, and 310 nmol mol^{-1} N_2O. The pressure and temperature of the sample were 740 Torr and 305 K, respectively. A set of 30 single-beam spectra of this sample was collected over a 4-h period, each spectrum consisting of 256 coadded scans and taking 8 min to collect. These were converted to absorbance spectra with reference to a 256-scan spectrum of the evacuated White cell collected earlier. In a similar manner, four further sets of 30 absorbance spectra were collected, consisting of 128- (4 min collection time), 64- (2 min), 32- (1 min), and 16-scan spectra (0.5 min), respectively. All of these spectra were analyzed using the CLS prediction procedure. Thus, each set of spectra provided four sets of 30 trace gas concentrations, one set each for CO_2, CH_4, CO, and N_2O.

After accounting for a slow linear instrument drift due to a change in the laboratory temperature, the precision of the analyses (one standard deviation) for each of the four species was determined for the 256-scan experiment, the 128-scan experiment, and so on. The results of this set of experiments are plotted as solid squares separately for the four species concentrations in Figure 8. Figure 8 illustrates analytical precision (expessed as SEP) in both absolute and percentage terms as a function of the number of coadded scans in the spectra.

The same experiment was repeated, except that the sample was changed between measurements to assess the effects of sample handling on precision. The same tank of calibrated well-characterized air was used. Sample pressure and temperature were maintained at 760 Torr and 306 K, respectively. After each analysis, the White cell was evacuated and then refilled from the tank via the sampling manifold, the whole process automated by a computer program. A set of 32 consecutive 256-scan spectra was collected in this way, as well as a set of 40 consecutive 64-scan spectra and a set of 12 32-scan spectra. These were analyzed in the same manner as described above. The level of analytical precision achieved in this experiment, involving sample handling, plotted as open triangles in Figure 8, was essentially the same as that achieved in the experiment not involving sample handling. This confirms that the analytical precision is not currently limited by sample handling.

Application to Atmospheric Monitoring. The spectrometer, fitted with the 22-m White cell, was temporarily installed at the Cape Grim Baseline Air Pollution Station (CGBAPS), on the northwest coast of Tasmania. The station is part of a global network of atmospheric monitoring stations. The instrument was programmed to draw in a sample of the atmosphere, and record an absorbance spectrum of the air sample, every 30 min over a period of about five weeks. These spectra were analyzed in real time to provide a record of CO_2, CH_4, N_2O, and CO mixing ratios. The calibrated mixing ratio ranges, and the calibration windows used were

$$340 < CO_2 < 380\ \mu\text{mol mol}^{-1}, \quad 2020-2310\ \text{cm}^{-1}$$

$$1680 < CH_4 < 1750\ \text{nmol mol}^{-1}, \quad 2810-3150\ \text{cm}^{-1}$$

$$40 < CO < 100\ \text{nmol mol}^{-1}, \quad 2050-2220\ \text{cm}^{-1}$$

$$310 < N_2O < 320\ \text{nmol mol}^{-1}, \quad 2020-2265\ \text{cm}^{-1}$$

These concentration ranges, although relatively narrow, were appropriate for the monitoring of Southern Hemisphere maritime boundary layer air at a baseline station. Few excursions beyond these ranges were observed. Every 6 h, a sample of air from a calibration tank containing well-characterized clean air (with CO_2, CH_4, CO, and N_2O mixing ratios assigned by GASLAB) was analyzed, to provide an absolute calibration for the FT-IR analyses. This calibration enabled the FT-IR data to be reported with reference to the GASLAB mixing ratio scales. Figure 9a illustrates the mixing ratio record for the four trace gases over a five-week period. Also illustrated are the parallel mixing ratio data acquired by routine instruments at CGBAPS, gas chromatography for CH_4, N_2O, and CO and by NDIR for CO_2, also reported on the GASLAB mixing ratio scales. The CH_4, N_2O, and CO GC data were provided by the Advanced Global Atmospheric Gases Experiment (AGAGE) program.[22] Figure 9b shows a five-day period within this time characterized by continuous baseline (clean air) conditions. The FT-IR data exhibited a level of analytical precision and accuracy similar to that attainable using the conventional techniques employed by the AGAGE instrument. The levels of analytical precision and accuracy attained using FT-IR spectroscopy in this application are listed in Table 2. (For CH_4, N_2O, and CO these are slightly superior to those shown in Figure 8, where the 9.8-m White cell was used. The longer path length of the 22-m White cell allows a somewhat greater absorbance relative to noise to be obtained, which translates directly into better measurement precision.)

Table 2.[a] Modeled and Experimental Analytical Precision

SEP	approx mixing ratio	precision $\pm\sigma$ ($\pm\sigma$%)		FT-IR-NDIR or FT-IR-GC $\pm\Delta$ ($\pm\Delta$%)
		modeled	experimental	
CO_2 (μmol mol^{-1})	360	0.05 (0.014%)	0.15 (0.04%)	0.02 (0.006%)
CH_4 (nmol mol^{-1})	1700	0.6 (0.04%)	0.9 (0.05%)	0.5 (0.03%)
CO (nmol mol^{-1})	50	0.3 (0.6%)	0.27 (0.5%)	0.6 (1.0%)
N_2O (nmol mol^{-1})	310	0.1 (0.03%)	0.28 (0.1%)	0.4 (0.1%)

[a] The third column lists for each species, the modeled precision for spectroscopic noise levels equivalent to a 256-scan spectrum; the fourth column lists the experimental precision actually attained using 256 scans and 22 m. As an estimate of the accuracy of the FT-IR technique, the fifth column lists for each species the mean of the differences, Δ, between parallel measurements of the CO_2 mixing ratio by FT-IR and NDIR, and CH_4, CO, and N_2O by FT-IR and AGAGE-GC. The mean differences are expressed both in terms of molar fraction mixing ratios and as a percent of the mixing ratio of the species in Southern Hemisphere baseline air, as listed in the second column. For the fifth column instrument difference results, only data collected during baseline (clean air) conditions were considered.

MALT Modeling of Precision vs Noise. It is possible to compare the experimentally obtained analytical precision levels with purely MALT-modeled analytical precision levels. The modeled precision can be used to indicate the best performance obtainable in an ideal experiment. The difference between the modeled and the experimental analytical precision indicates how nearly the real measurement approaches the ideal.

The MALT program was used to calculate sets of validation spectra of air containing the trace gases in the mixing ratio ranges and spectral regions as listed above for the Cape Grim experiment. The MALT model also specified 1-cm^{-1} resolution, pressure of 760 Torr, temperature of 300 K, and path length of 22 m. The MALT spectra were calculated with a peak-to-peak absorbance noise level of 3.5×10^{-5} in the region of the spectrum where CO_2, CO, and N_2O are analyzed and $\sim 7 \times 10^{-5}$ in the CH_4 region. This is the noise level observed in a 256-scan spectrum of air under the conditions described above. A CLS calibration was generated with this set of spectra. For each species, the CLS calibration procedure provides the SEP as a measure of the precision of the calibration (see equation).

The MALT-modeled SEP results determined here and the corresponding experimental precision results, reported immedi-

(22) Steele, L. P.; Lucarelli, M. P.; Fraser, P. J.; Derek, N.; Porter, L. W. In *Baseline Atmospheric Program Australia 1994−95*; Francey, R. J., Dick, A. L., Derek, N., Eds.; Bureau of Meteorology and CSIRO Division of Atmospheric Research: Melbourne, 1996; pp 134−140.

ately above, are summarized in Table 2. Comparing the modeled and experimental precision results, it is generally the case that the MALT/CLS model is a broad guide (to within a factor of 3) to what we have achieved in practice. For CO_2 and N_2O, the experimental precision was never better than a third of that of the model. For CO_2, we suspect that this is attributable to the strong and slightly Beer−Lambert nonlinear absorbance of some of the $^{12}CO_2$ lines included in the calibration window. For N_2O, we suspect that the discrepancy between model and experiment is due to the CLS prediction algorithm not being entirely successful in distinguishing between the broad featureless N_2O band and low-frequency baseline fluctuations in the N_2O region which are a feature of experimental spectra but not of MALT spectra.

The implications of this predictive capability of the MALT/CLS model are important. The MALT program combined with the CLS calibration and prediction processes as described above can serve as a virtual experimental platform, allowing systematic optimization of the many experimental parameters and tradeoffs to be performed before any samples are measured on a spectrometer.

CONCLUSION

We have described a novel method of precise and accurate trace gas analysis using FT-IR spectroscopy. The method is applied to whole air samples, the only pretreatment usually required being drying. Simultaneous analysis of CO_2, CH_4, CO, and N_2O mixing ratios in air was achieved. The precision of the mixing ratio retrievals was of the order of 0.1% for CO_2, CH_4, and N_2O and 0.5% for CO at clean air levels. With calibration against a reference gas, the method offers accuracy to within its limits of precision. The analysis is carried out on a benchtop, 1-cm^{-1} instrument which is deployable in field studies. It has also been demonstrated that the MALT program allows the modeling an FT-IR experiment without having to perform it. The influence of various experimental parameters may be investigated and the experiment optimized first on a virtual platform, offering economies in both time and resources. The results returned by the modeling exercise offer realistic estimates as to what may be achieved by actual experiment. The method described here for trace gas mixing ratio analysis is, in the companion paper,[11] expanded and refined to allow the determination of the stable isotope ratio $^{13}C/^{12}C$ in CO_2. The potential for broader application to other geophysically important stable isotope ratio analyses is considered.

ACKNOWLEDGMENT

We thank the staff of GASLAB, and in particular Ray Langenfelds, for the provision of calibration gases used in this work; L. Porter and other CGBAPS staff for assistance at Cape Grim; and the AGAGE program for early access to some of their data. M.B.E. thanks CSIRO Atmospheric Research and the Bureau of Meteorology (through CGBAPS) for research and living support, and the Australian Academy of Science for a travel grant.

Received for review May 25, 1999. Accepted September 21, 1999.

AC9905625